

Triply degenerate nodal line and tunable contracted-drumhead surface state in a tight-binding model

Yi-Ru Wang and Gui-Bin Liu*

Centre for Quantum Physics, Key Laboratory of Advanced Optoelectronic Quantum Architecture and Measurement (MOE),
School of Physics, Beijing Institute of Technology, Beijing 100081, China and
Beijing Key Laboratory of Nanophotonics and Ultrafine Optoelectronic Systems,
School of Physics, Beijing Institute of Technology, Beijing 100081, China

The study of topological semimetals has been extended to more general topological nodal systems such as metamaterials and artificial periodic structures. Among various nodal structures, triply degenerate nodal line (TNL) is rare and hence lack of attention. In this work, we have proposed a simple tight-binding model which hosts a topological non-trivial TNL. This TNL not only has the drumhead surface states as usual nodal line systems, but also has surface states which form a contracted-drumhead shape. And the shape and area of this contracted-drumhead can be tuned by the hopping parameters of the model. This provides an effective way to modulate surface states as well as their density of states, which can be important in future applications of topological nodal systems.

I. INTRODUCTION

In recent years, topological semimetals have become a frontier topic in condensed matter physics because of their promising applications in electronics, spintronics, and optics [1–9]. According to the dimensions of the degenerate manifolds in k -space formed by band crossings, topological semimetals are divided into nodal point semimetals such as Weyl [9–12], Dirac [13–17], or triple point semimetals [18, 19], nodal line semimetals [20–23], and nodal surface semimetals [24–27]. Due to the non-trivial topological band structure, Weyl (Dirac) semimetals can exhibit Fermi arc surface states [5, 9, 10] connecting different Weyl-node (Dirac-node) projections on a two-dimensional (2D) surface Brillouin zone (BZ), and nodal line semimetals can exhibit another special surface state — drumhead surface state (DSS) [21, 22, 28–31] on a 2D surface BZ. In fact, these non-trivial topological properties are not limited to being present in semimetals, because they originate from the nodal band structures and they also exist in other systems such as metals [32–35], optical crystals [36–38], phononic crystals [39, 40], mechanical systems [41], and circuit systems [42–44].

For topological nodal line materials, doubly degenerate Weyl nodal line [23, 45–47] and quadruply degenerate Dirac nodal line [48–51] have been broadly studied, and the DSS has been observed in both these two kinds of materials. However, about triply degenerate nodal line (TNL), there is very little research on it. The only such research we can find is Ref. [52] by Liu *et al.* in 2021. In Ref. [52], two TNL models were proposed, one of which is nontopological and the other is topological according to the existence of Fermi arc topological surface states. However, no DSS was reported for the TNL models in Ref. [52]. Accordingly, in this work we aim to construct a tight-binding (TB) model with TNL and investigate its

DSS.

However, it's almost impossible to construct a TNL model based on real crystalline materials, because real crystalline materials are constrained by the symmetries of (magnetic) space groups and systematic studies on the possible emergent particles from band crossings have shown that no TNL exists under various (magnetic) space groups [53–55]. Then, to construct a TNL model one has to get rid of the constraints by (magnetic) space groups. This can be achieved in artificial systems such as metamaterials, circuit systems, and mechanical systems, because when described by TB models the effective hoppings in these systems can be tuned at will, e.g. adjusting the connection mode among circuit components or changing the coupling strength through springs [41, 43, 56].

In this work, we first constructed a three-band TB model hosting TNL by designing the hoppings. Then, we calculated the Berry phase and Zak phase to check the topological non-triviality of the TNL. Surface states on two different surfaces, i.e. (010) and ($\bar{1}$ 10), were studied via both semi-infinite systems and slab models. The usual DSS was found on the (010) surface. However, on the ($\bar{1}$ 10) surface we noticed a new kind of DSS, whose drumhead is not a complete one but a contracted one. The tuning of this DSS with contracted drumhead was also studied by varying the hopping parameters of the model.

II. MODEL AND METHOD

The model is constructed based on a simple cubic lattice whose basis vectors \vec{a} , \vec{b} , and \vec{c} are equal in magnitude and along x , y , and z direction respectively, as shown in Fig. 1(a). Only one atom with three orbitals (here called ϕ_1 , ϕ_2 , ϕ_3) is considered in each cell. With the hopping between orbitals $\phi_i(\vec{r})$ and $\phi_j(\vec{r} - \vec{a})$ denoted as $h_{ij}(\vec{a})$, we choose the following hoppings for the model.

$$h_{11}(0) = t_0, \quad h_{22}(0) = -t_0, \quad h_{33}(0) = 2t_0 \quad (1)$$

* Corresponding author: gbliu@bit.edu.cn

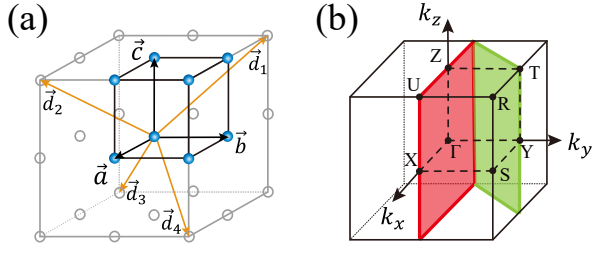


FIG. 1. (a) Unit cell (black) and hopping vectors of the model. (b) The bulk BZ and its projections to (010) surface (red) and (110) surface (green).

$$h_{11}(\pm\alpha) = \frac{t_1}{2}, \quad h_{22}(\pm\alpha) = -\frac{t_1}{2}, \quad h_{33}(\pm\alpha) = t_1 \quad (2)$$

$$h_{23}(\pm\vec{b}) = \pm\frac{t_2}{2}, \quad h_{12}(\pm\vec{d}_i) = \pm\frac{t_3}{8} \quad (i = 1, 2, 3, 4) \quad (3)$$

in which $\alpha = \vec{a}, \vec{b}, \vec{c}$. Then the Hamiltonian of the TB model is

$$H = (t_0 + t_1 \cos k_x + t_1 \cos k_y + t_1 \cos k_z)\lambda_1 + t_2 \sin k_y \lambda_2 + t_3 \sin k_x \sin k_y \sin k_z \lambda_3 \quad (4)$$

in which λ_1, λ_2 , and λ_3 are the following three matrices respectively:

$$\begin{pmatrix} 1 & 0 & 0 \\ 0 & -1 & 0 \\ 0 & 0 & 2 \end{pmatrix}, \quad \begin{pmatrix} 0 & 0 & 0 \\ 0 & 0 & i \\ 0 & -i & 0 \end{pmatrix}, \quad \begin{pmatrix} 0 & i & 0 \\ -i & 0 & 0 \\ 0 & 0 & 0 \end{pmatrix}. \quad (5)$$

One can easily see that, when $k_y = 0$, Eq. (4) becomes a diagonal matrix whose diagonal elements can be null simultaneously. This implies that a TNL can exist in the plane $k_y = 0$ under suitable values of t_0 and t_1 . The key feature of the hoppings that results in this TNL is that $h_{ii}(0)/h_{ii}(\pm\alpha)$ keeps constant for $i = 1, 2, 3$. This is a special request that cannot be derived from symmetries of (magnetic) space group.

The surface density of state (SDOS) was obtained by calculating the surface Green's function of semi-infinite system using the Wanniertools package [57]. The input data for Wanniertools was prepared by the MagneticTB package [58]. To investigate the surface states, we also constructed TB slab models of 80 layers using the PythTB package [59]. In order to judge whether a state is a surface state, we first define the topmost five layers on each side, A or B, of the slab model as "surface layers", and then define the following quantity η to characterize the degree to which a state is a surface state

$$\eta = \begin{cases} [w_A + w_B - \frac{1}{8}]/\frac{7}{8}, & w_A + w_B > \frac{1}{8} \\ 0, & w_A + w_B \leq \frac{1}{8} \end{cases} \quad (6)$$

where $w_{A/B}$ represents the wavefunction weight within the surface layers of side A/B of the slab. For a bulk

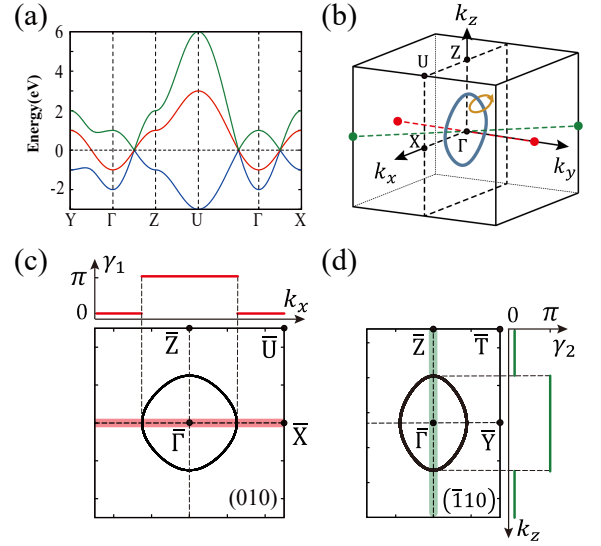


FIG. 2. (a) The bulk band structure of the model. (b) The TNL (thick blue nodal ring) and the k -point path (small orange loop) for calculating the Berry phase. The red (green) dashed line is the integral path for Zak phase γ_1 at $k_x = 0$ (γ_2 at $k_z = 0$). (c,d) The TNL projections onto (c) (010) and (d) (110) surface BZs, and the Zak phases (c) $\gamma_1(k_x)$ and (d) $\gamma_2(k_z)$.

state wavefunction, it is periodic and its weights are equally distributed within all the 80 layers, in which case $w_A = w_B = 5/80$ and $\eta = 0$. For a perfect surface state, wavefunction is totally localized within the surface layers, leading to $w_A = w_B = 1/2$ and $\eta = 1$. By means of η , a state can be determined as a strong (or typical) surface state if its η is greater than a critical value η_c and in this paper $\eta_c = 0.5$ is adopted.

III. RESULTS

If not otherwise stated, the parameters $t_0 = 2$, $t_1 = -1$, and $t_2 = t_3 = 1$ are used for the model and the unit is eV for all energies. The bulk energy bands are shown in Fig. 2(a) in which the k points are defined in Fig. 1(b). In this model, the TNL is actually an approximately circular nodal ring in the $k_y = 0$ plane, as shown in Fig. 2(b). To check the topological properties of the TNL, we first calculated the Berry phase defined on a closed k -point loop enclosing the TNL, with fully gapped energies, as shown by the small orange loop in Fig. 2(b). The Berry phase is calculated using the Wilson loop approach [60] and the result is π , which shows the topological non-triviality of the TNL.

Besides, we also calculated the Zak phase [61, 62], which is the Berry phase defined in a one-dimensional BZ along a certain direction. Two Zak phases are investigated here. The first one $\gamma_1(k_x)$ is defined along the line from $(k_x, -\frac{1}{2}, 0)$ to $(k_x, \frac{1}{2}, 0)$ with the $k_x = 0$

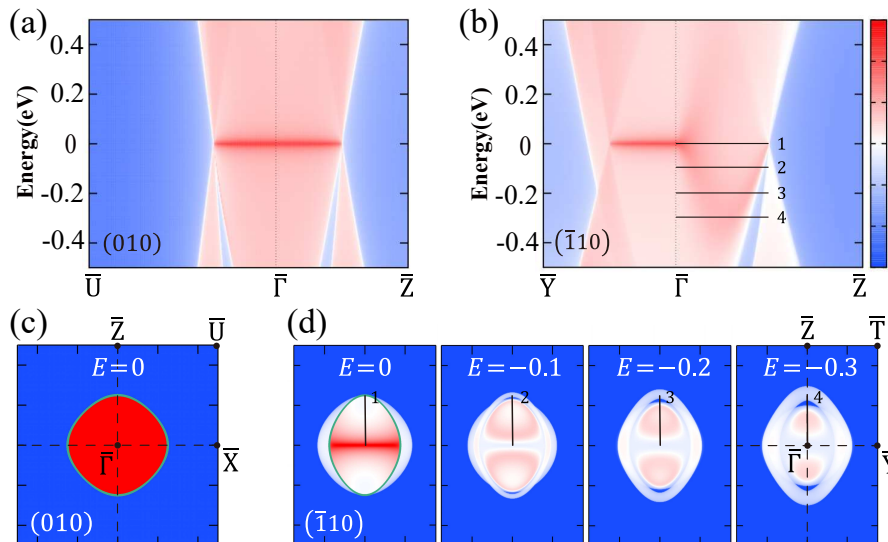


FIG. 3. Topological surface states given by SDOS for the semi-infinite systems terminated with (a,c) (010) and (b,d) ($\bar{1}10$) surfaces. (a,b) Continuous energy resolved SDOS. (c) The constant energy slice at $E = 0$ for the (010) surface system. (d) The constant energy slices at $E = 0, -0.1, -0.2, -0.3$ for the ($\bar{1}10$) surface system, in which the cutting lines 1–4 correspond to the ones in (b). The green lines in (c,d) are the projections of the TNL.

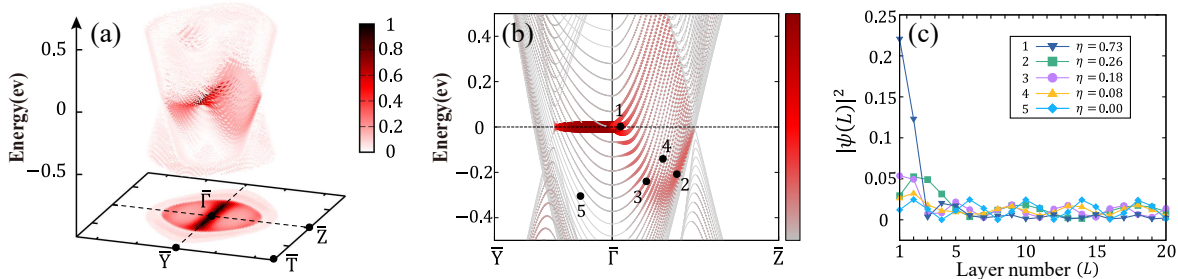


FIG. 4. The ($\bar{1}10$) slab model. (a) The distribution of η (the degree of surface state) represented by color for all states with energy in the range $[-0.5, 0.5]$. The largest η at each k -point is also projected onto the surface BZ. (b) Energy bands with η represented by both color and the point size. (c) The squared wavefunctions with respect to the layer number (only 20 out of the total 80 layers are shown) for the five states marked in (b).

case shown by the red dashed line in Fig. 2(b), in which the k -point coordinates are in unit of $2\pi/a$. The second one $\gamma_2(k_z)$ is defined along the line from $(\frac{1}{2}, -\frac{1}{2}, k_z)$ to $(-\frac{1}{2}, \frac{1}{2}, k_z)$ with the $k_z = 0$ case shown by the green dashed line in Fig. 2(b). The calculated Zak phase $\gamma_1(k_x)$ ($\gamma_2(k_z)$) is shown in the top (right) panel of Fig. 2(c) (Fig. 2(d)) whose k_x (k_z) axis corresponds to the red (green) thick line in the 2D projective BZ of (010) ($\bar{1}10$) surface shown in the corresponding bottom (left) panel. We can see that, for both γ_1 and γ_2 , the non-trivial π Zak phase emerges only when the integral path of Zak phase traverses the nodal ring, i.e. the TNL here; otherwise the Zak phase is zero. According to the bulk-edge correspondence [63], this change of topological properties from inside to outside the nodal ring implies the existence of topological surface states inside the projected nodal ring on both (010) and ($\bar{1}10$) surfaces.

To explore the topological surface states of a certain surface, the semi-infinite system terminated with that surface should be constructed. Two surfaces (010) and ($\bar{1}10$) are studied here, where the (010) surface is parallel to the nodal ring but the ($\bar{1}10$) surface is not. Fig. 3(a) shows the SDOS of the (010) surface system, whose surface states all have a constant energy (zero) and form a flat drumhead shape. This typical DSS is clearly demonstrated by the SDOS with constant energy slice at $E = 0$, as shown in Fig. 3(c). The green ring in Fig. 3(c) represents the front projection of the TNL, and its interior is full of surface states. We call this kind of DSS as “full DSS”. From the result that both the Zak phases γ_1 and γ_2 equal π inside the TNL projections, one may expect that full DSS also exists in the ($\bar{1}10$) surface system. However, the SDOS of the ($\bar{1}10$) surface system shown in Fig. 3(b) and (d) demonstrates results different from

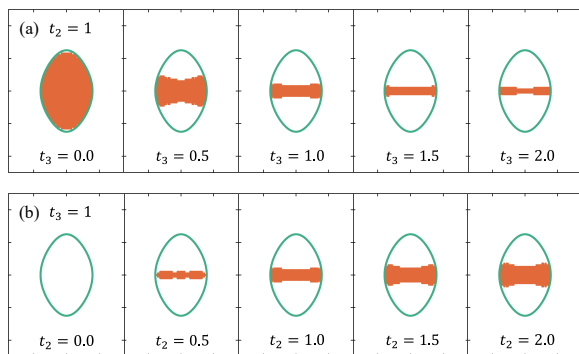


FIG. 5. The k -point distribution (orange area) of the CDSS for the $(\bar{1}10)$ slab model with different parameters. (a) $t_3 = 0, 0.5, 1.0, 1.5, 2.0$ with $t_2 = 1.0$. (b) $t_2 = 0, 0.5, 1.0, 1.5, 2.0$ with $t_3 = 1.0$. The green ellipse denotes the projection of the TNL. Other two parameters are $t_0 = 2$ and $t_1 = -1$ for all cases.

the expectation. Especially, the leftmost panel of Fig. 3(d) shows “contracted-drumhead surface state (CDSS)”, in which the surface states do not fill completely the interior of the TNL oblique projection (the green ellipse). The weak surface state feature at other energies as shown in other panels of Fig. 3(d) also supports this result.

To further explore the CDSS in the $(\bar{1}10)$ surface system, a slab model of 80 layers terminated with $(\bar{1}10)$ surface is studied and its energy bands are shown in Fig. 4(b), in which the degree of surface state η defined in Eq. (6) is also shown by both the point size and color for each state. In addition, Fig. 4(a) shows the distribution of η for all states within the energy range $[-0.5, 0.5]$ in the whole surface BZ and the projection of η onto the surface BZ. Fig. 4(b) corresponds to Fig. 3(b), but here we can access the wavefunction of any state of the slab model. The wavefunctions of the five states marked in Fig. 4(b) have descending η from 0.73 to 0 and the distributions of their weights with respect to layer number are given in Fig. 4(c). We can see that the state 1 with $\eta = 0.73$ is a strong surface state with most wavefunction localized within the surface layers. At the other extreme, state 5 with $\eta = 0$ distributes periodically and hence is a bulk state. As for the states 2–4, they have nonzero but small η . Although they contain surface state components

or may be called weak surface states, they are more like bulk states. From Figs. 4(a) and 4(b) we can see that strong surface states exist only near zero energy. Consequently, even if the projection of η in Fig. 4(a) selects the largest η for each k -point within the energy range $[-0.5, 0.5]$, it is not much different from the case considering only zero energy and it exhibits similar shape to the $E = 0$ panel in Fig. 3(d).

Because the weak surface states are much like bulk states, they are not efficient in most applications which require large SDOS. Thus, only strong surface states need to be considered, and the shape of the CDSS can be revealed by the distribution of the k -points at which strong surface states exist. Fig. 5 shows the distribution of the k -points of strong surface states, i.e. the shape of CDSS, under different model parameters. We can see that the shape of CDSS for the $(\bar{1}10)$ surface can be tuned by the hoppings t_2 and t_3 efficiently, namely, increasing t_3 makes the surface states changing from a full DSS to a CDSS with smaller and smaller areas (Fig. 5(a)), and inversely, increasing t_2 will increase the area of CDSS from zero (Fig. 5(b)). This provides an effective route to tune the SDOS and the shape of surface state in topological nodal systems.

IV. CONCLUSIONS

In summary, we have proposed a simple TB model hosting TNL and studied its topological properties. Both Berry phase and Zak phase demonstrate that the TNL is topological non-trivial. This TNL model not only has a full DSS as usual topological nodal line systems, but also has a CDSS which we first noticed. The CDSS exists on the $(\bar{1}10)$ surface and its area can be tuned efficiently by both the model parameters t_2 and t_3 . Our model demonstrates an effective way to tune the amount and density of states of the surface states, which will expand the potential applications of topological nodal line systems.

V. ACKNOWLEDGMENTS

This work is supported by the National Natural Science Foundation of China with Grant Nos. 12274028, 52161135108, and 12234003 and the National Key R&D Program of China with Grant No. 2022YFA1402603.

-
- [1] A. Bansil, H. Lin, and T. Das, *Rev. Mod. Phys.* **88**, 021004 (2016).
 - [2] H. M. Weng, X. Dai, and Z. Fang, *J. Phys. Condens. Matter* **28**, 303001 (2016).
 - [3] A. A. Burkov, M. D. Hook, and L. Balents, *Phys. Rev. B* **84**, 235126 (2011).
 - [4] B. H. Yan and C. Felser, *Annu. Rev. Condens. Matter Phys.* **8**, 337 (2017).
 - [5] M. Z. Hasan, S. Y. Xu, I. Belopolski, and S. M. Huang, *Annu. Rev. Condens. Matter Phys.* **8**, 289 (2017).
 - [6] W. Witczak-Krempa, G. Chen, Y. B. Kim, and L. Balents, *Annu. Rev. Condens. Matter Phys.* **5**, 57 (2014).
 - [7] B. A. Bernevig, C. Felser, and H. Beidenkopf, *Nature* **603**, 41 (2022).
 - [8] B. Q. Lv, T. Qian, and H. Ding, *Rev. Mod. Phys.* **93**, 025002 (2021).

- [9] X. Wan, A. M. Turner, A. Vishwanath, and S. Y. Savrasov, *Phys. Rev. B* **83**, 205101 (2011).
- [10] H. M. Weng, C. Fang, Z. Fang, B. A. Bernevig, and X. Dai, *Phys. Rev. X* **5**, 011029 (2015).
- [11] S.-Y. Xu, I. Belopolski, N. Alidoust, M. Neupane, G. Bian, C. Zhang, R. Sankar, G. Chang, Z. Yuan, C.-C. Lee, S.-M. Huang, H. Zheng, J. Ma, D. S. Sanchez, B. Wang, A. Bansil, F. Chou, P. P. Shibayev, H. Lin, S. Jia, and M. Z. Hasan, *Science* **349**, 613 (2015).
- [12] S.-Y. Xu, N. Alidoust, I. Belopolski, Z. Yuan, G. Bian, T.-R. Chang, H. Zheng, V. N. Strocov, D. S. Sanchez, G. Chang, C. Zhang, D. Mou, Y. Wu, L. Huang, C.-C. Lee, S.-M. Huang, B. Wang, A. Bansil, H.-T. Jeng, T. Neupert, A. Kaminski, H. Lin, S. Jia, and M. Z. Hasan, *Nat. Phys.* **11**, 748 (2015).
- [13] Z. Wang, Y. Sun, X.-Q. Chen, C. Franchini, G. Xu, H. Weng, X. Dai, and Z. Fang, *Phys. Rev. B* **85**, 195320 (2012).
- [14] Z. Wang, H. Weng, Q. Wu, X. Dai, and Z. Fang, *Phys. Rev. B* **88**, 125427 (2013).
- [15] Z. K. Liu, B. Zhou, Y. Zhang, Z. J. Wang, H. M. Weng, D. Prabhakaran, S.-K. Mo, Z. X. Shen, Z. Fang, X. Dai, Z. Hussain, and Y. L. Chen, *Science* **343**, 864 (2014).
- [16] Z. K. Liu, J. Jiang, B. Zhou, Z. J. Wang, Y. Zhang, H. M. Weng, D. Prabhakaran, S.-K. Mo, H. Peng, P. Dudin, T. Kim, M. Hoesch, Z. Fang, X. Dai, Z. X. Shen, D. L. Feng, Z. Hussain, and Y. L. Chen, *Nat. Mater.* **13**, 677 (2014).
- [17] M. Neupane, S.-Y. Xu, R. Sankar, N. Alidoust, G. Bian, C. Liu, I. Belopolski, T.-R. Chang, H.-T. Jeng, H. Lin, A. Bansil, F. Chou, and M. Z. Hasan, *Nat Comms* **5**, 3786 (2014).
- [18] B. Q. Lv, Z.-L. Feng, Q.-N. Xu, X. Gao, J.-Z. Ma, L.-Y. Kong, P. Richard, Y.-B. Huang, V. N. Strocov, C. Fang, H.-M. Weng, Y.-G. Shi, T. Qian, and H. Ding, *Nature* **546**, 627 (2017).
- [19] J.-Z. Ma, J.-B. He, Y.-F. Xu, B. Q. Lv, D. Chen, W.-L. Zhu, S. Zhang, L.-Y. Kong, X. Gao, L.-Y. Rong, Y.-B. Huang, P. Richard, C.-Y. Xi, E. S. Choi, Y. Shao, Y.-L. Wang, H.-J. Gao, X. Dai, C. Fang, H.-M. Weng, G.-F. Chen, T. Qian, and H. Ding, *Nat. Phys.* **14**, 349 (2018).
- [20] C. Fang, Y. Chen, H.-Y. Kee, and L. Fu, *Phys. Rev. B* **92**, 081201 (2015).
- [21] H. Huang, J. Liu, D. Vanderbilt, and W. Duan, *Phys. Rev. B* **93**, 201114 (2016).
- [22] Q. Xu, R. Yu, Z. Fang, X. Dai, and H. Weng, *Phys. Rev. B* **95**, 045136 (2017).
- [23] W. Chen, H. Z. Lu, and J. M. Hou, *Phys. Rev. B* **96**, 041102 (2017).
- [24] W. Wu, Y. Liu, S. Li, C. Zhong, Z.-M. Yu, X.-L. Sheng, Y. X. Zhao, and S. A. Yang, *Phys. Rev. B* **97**, 115125 (2018).
- [25] B.-B. Fu, C.-J. Yi, T.-T. Zhang, M. Caputo, J.-Z. Ma, X. Gao, B. Q. Lv, L.-Y. Kong, Y.-B. Huang, P. Richard, M. Shi, V. N. Strocov, C. Fang, H.-M. Weng, Y.-G. Shi, T. Qian, and H. Ding, *Sci. Adv.* **5**, eaau6459 (2019).
- [26] Y. Yang, J. ping Xia, H. xiang Sun, Y. Ge, D. Jia, S. qi Yuan, S. A. Yang, Y. Chong, and B. Zhang, *Nat. Commun.* **10**, 5185 (2019).
- [27] S.-Z. Chen, S. Li, Y. Chen, and W. Duan, *Nano Lett.* **20**, 5400 (2020).
- [28] H. M. Weng, Y. Y. Liang, Q. N. Xu, R. Yu, Z. Fang, X. Dai, and Y. Kawazoe, *Phys. Rev. B* **92**, 045108 (2015).
- [29] Y. H. Chan, C. K. Chiu, M. Y. Chou, and A. P. Schnyder, *Phys. Rev. B* **93**, 205132 (2016).
- [30] G. Bian, T.-R. Chang, H. Zheng, S. Velury, S.-Y. Xu, T. Neupert, C.-K. Chiu, S.-M. Huang, D. S. Sanchez, I. Belopolski, N. Alidoust, P.-J. Chen, G. Chang, A. Bansil, H.-T. Jeng, H. Lin, and M. Z. Hasan, *Phys. Rev. B* **93**, 121113 (2016).
- [31] I. Belopolski, K. Manna, D. S. Sanchez, G. Chang, B. Ernst, J. Yin, S. S. Zhang, T. Cochran, N. Shumiya, H. Zheng, B. Singh, G. Bian, D. Multer, M. Litskevich, X. Zhou, S.-M. Huang, B. Wang, T.-R. Chang, S.-Y. Xu, A. Bansil, C. Felser, H. Lin, and M. Z. Hasan, *Science* **365**, 1278 (2019).
- [32] S.-Y. Xu, C. Liu, S. K. Kushwaha, R. Sankar, J. W. Krizan, I. Belopolski, M. Neupane, G. Bian, N. Alidoust, T.-R. Chang, H.-T. Jeng, C.-Y. Huang, W.-F. Tsai, H. Lin, P. P. Shibayev, F.-C. Chou, R. J. Cava, and M. Z. Hasan, *Science* **347**, 294 (2015).
- [33] Z. Wang, D. Gresch, A. A. Soluyanov, W. Xie, S. Kushwaha, X. Dai, M. Troyer, R. J. Cava, and B. A. Bernevig, *Phys. Rev. Lett.* **117**, 056805 (2016).
- [34] Z. Zhu, G. W. Winkler, Q. Wu, J. Li, and A. A. Soluyanov, *Phys. Rev. X* **6**, 031003 (2016).
- [35] J.-P. Sun, D. Zhang, and K. Chang, *Phys. Rev. B* **96**, 045121 (2017).
- [36] W. Gao, B. Yang, B. Tremain, H. Liu, Q. Guo, L. Xia, A. P. Hibbins, and S. Zhang, *Nat. Commun.* **9**, 950 (2018).
- [37] B. Yang, Q. Guo, B. Tremain, R. Liu, L. E. Barr, Q. Yan, W. Gao, H. Liu, Y. Xiang, J. Chen, C. Fang, A. Hibbins, L. Lu, and S. Zhang, *Science* **359**, 1013 (2018).
- [38] L. Wang, S.-K. Jian, and H. Yao, *Phys. Rev. A* **93**, 061801 (2016).
- [39] F. Li, X. Huang, J. Lu, J. Ma, and Z. Liu, *Nat. Phys.* **14**, 30 (2017).
- [40] T. Zhang, Z. Song, A. Alexandradinata, H. Weng, C. Fang, L. Lu, and Z. Fang, *Phys. Rev. Lett.* **120**, 016401 (2018).
- [41] G. C. Ma, M. Xiao, and C. T. Chan, *Nat. Rev. Phys.* **1**, 281 (2019).
- [42] Y. H. Lu, N. Y. Jia, L. Su, C. Owens, G. Juzeliūnas, D. I. Schuster, and J. Simon, *Phys. Rev. B* **99**, 020302 (2019).
- [43] C. H. Lee, S. Imhof, C. Berger, F. Bayer, J. Brehm, L. W. Molenkamp, T. Kiessling, and R. Thomale, *Commun. Phys.* **1**, 39 (2018).
- [44] K. Luo, R. Yu, and H. Weng, *Research* **2018**, 6793752 (2018).
- [45] B. J. Feng, R. W. Zhang, Y. Feng, B. T. Fu, S. L. Wu, K. Miyamoto, S. L. He, L. Chen, K. H. Wu, K. Shimada, T. Okuda, and Y. G. Yao, *Phys. Rev. Lett.* **123**, 116401 (2019).
- [46] L. L. Liu, C. Z. Wang, J. X. Li, X. Q. Chen, Y. Jia, and J. H. Cho, *Phys. Rev. B* **101**, 165403 (2020).
- [47] C. Chen, Z. M. Yu, S. Li, Z. Y. Chen, X. L. Sheng, and S. A. Yang, *Phys. Rev. B* **99**, 075131 (2019).
- [48] Y. Kim, B. J. Wieder, C. L. Kane, and A. M. Rappe, *Phys. Rev. Lett.* **115**, 036806 (2015).
- [49] M. Nakhaee, S. A. Ketabi, and F. M. Peeters, *Phys. Rev. B* **98**, 115413 (2018).
- [50] R. H. Li, H. Ma, X. Y. Cheng, S. L. Wang, D. Z. Li, Z. Y. Zhang, Y. Y. Li, and X. Q. Chen, *Phys. Rev. Lett.* **117**, 096401 (2016).
- [51] K. Mullen, B. Uchoa, and D. T. Glatzhofer, *Phys. Rev. Lett.* **115**, 026403 (2015).

- [52] Z. H. Liu, L. Y. Wang, and D. X. Yao, *Phys. Rev. B* **103**, 205145 (2021).
- [53] Z.-M. Yu, Z. Zhang, G.-B. Liu, W. Wu, X.-P. Li, R.-W. Zhang, S. A. Yang, and Y. Yao, *Sci. Bull.* **67**, 375 (2022).
- [54] G.-B. Liu, Z. Zhang, Z.-M. Yu, S. A. Yang, and Y. Yao, *Phys. Rev. B* **105**, 085117 (2022).
- [55] Z. Zhang, G.-B. Liu, Z.-M. Yu, S. A. Yang, and Y. Yao, *Phys. Rev. B* **105**, 104426 (2022).
- [56] K. F. Luo and R. Yu, *Acta Phys. Sin.* **68**, 220305 (2019).
- [57] Q. S. Wu, S. N. Zhang, H. F. Song, M. Troyer, and A. A. Soluyanov, *Comput. Phys. Commun.* **224**, 405 (2018).
- [58] Z. Y. Zhang, Z. M. Yu, G. B. Liu, and Y. G. Yao, *Comput. Phys. Commun.* **270**, 108153 (2022).
- [59] I. Y. Tahir, V. David, and C. Sinisa, *Tight-binding formalism in the context of the pythtb package* (2022).
- [60] H. X. Wang, G. Y. Guo, and J. H. Jiang, *New J. Phys.* **21**, 093029 (2019).
- [61] J. Zak, *Phys. Rev. Lett.* **62**, 2747 (1989).
- [62] D. Xiao, M.-C. Chang, and Q. Niu, *Rev. Mod. Phys.* **82**, 1959 (2010).
- [63] J.-W. Rhim, J. Behrends, and J. H. Bardarson, *Phys. Rev. B* **95**, 035421 (2017).